J. Fluid Mech. (1980), *vol.* 917, *part* 4, *pp.* 771–781
Printed in Great Britain

A note on spanwise structure in the two-dimensional mixing layer

By F. K. BROWAND AND T. R. TROUTT

Department of Aerospace Engineering, University of Southern California, Los Angeles, California 90007

(Received 22 March 1979 and in revised form 31 August 1979)

The lateral extent of the large-scale features of a high-Reynolds-number, turbulent mixing layer are studied by means of an array of twelve hot wires placed across the span of the wind tunnel. Correlation measurements show that the large-scale structure rapidly approaches an asymptotic state, in which the lateral correlation length becomes proportional to the local mixing-layer thickness. Visualizations of the instantaneous hot-wire outputs show the large structure to extend across the wind tunnel, but to contain spanwise irregularities. It is argued that these spanwise irregularities are produced by the pairing interactions between adjacent vortices.

1. Introduction

There is considerable current interest in the two-dimensional turbulent mixing layer for several reasons. First, because this geometry is often found in nature, and is also characteristic of many technological applications, and, second, there is present in the mixing layer a seemingly organized, large-scale turbulent structure. The presence of this structure is now undisputed. Opinion is divided, however, as to its significance. Are these features transitional, and thus transitory, or do they persist indefinitely? Visual observations looking across the flow have shown structure at very large Reynolds numbers $O(10^7)$ (Dimotakis & Brown 1976). On the other hand, some plan-view smoke observations indicate that the structures are of limited spanwise extent (Chandrsuda *et al.* 1978). Is it possible that the strong lateral coherence observed visually early in the growth of the mixing layer becomes progressively weaker, and that the flow degenerates to a completely three-dimensional field with no indication of structure? There is evidence of a small-scale instability which produces lateral variation – the streaks observed by Brown & Roshko (1974). Can these smaller features be responsible for the presumed breakdown of the larger scales?

The recent work of Wygnanski *et al.* (1979) gives strong support for the persistence of the large-scale features by demonstrating high lateral correlation even in the presence of significant levels of free-stream turbulence, or with various tripping devices designed to make the initial mixing-layer turbulent. Important problems remain, however. These include the determination of the lateral scale associated with the large features, and the development of understanding concerning the scale change process which occurs as the structures convect downstream. In the present work we attempt to answer these questions using data obtained from a linear array of hot wires positioned across the span of a two-dimensional mixing layer.

0022-1120/80/4423-8730 $02.00

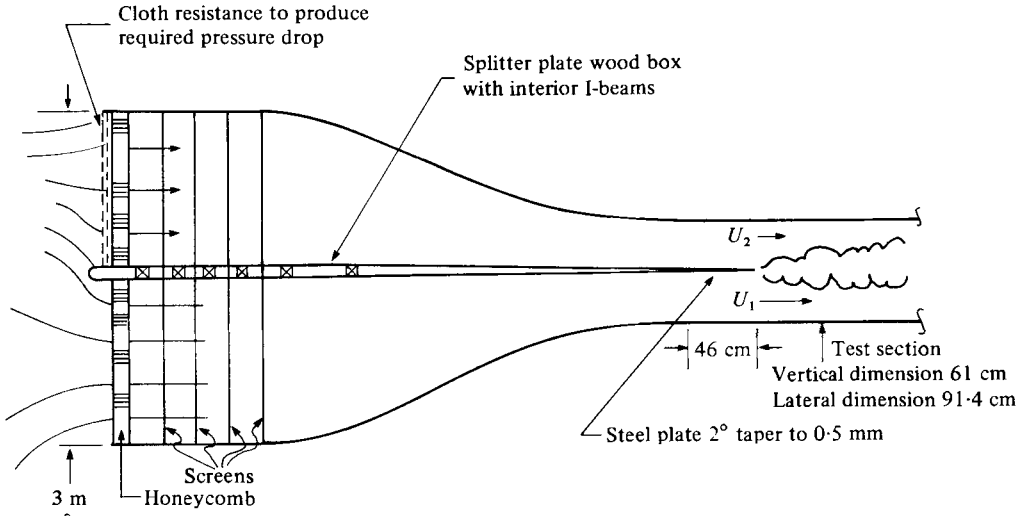

FIGURE 1. Schematic diagram of the wind tunnel.

2. Experimental arrangement and procedures

The experiments were performed in an open-return wind tunnel, specially constructed to study the two-dimensional mixing layer. The two streams are produced by dividing the stilling section into an upper and lower section independent from one another (see figure 1). A lower velocity is produced on the upper side by adding a cloth resistance at the front (upper half) of the tunnel. The velocity ratio used was nominally 8:1, and corresponds to $\lambda = (U_1 - U_2)/(U_1 + U_2) = 0{\cdot}8$. No tripping device was placed upon the splitter plate. The mixing layer was therefore allowed to undergo transition from an initially laminar boundary layer. The initial boundary layer and the characteristics of the mixing-layer growth have been carefully studied and appear in an earlier paper (see Browand & Latigo 1979).

Hot-wire measurements were made at six downstream locations between 4 cm and 92 cm from the plate trailing edge (figure 2). The Reynolds numbers corresponding to these locations varied from 3300 to 186000. Here Reynolds number is based upon the velocity difference and the maximum slope thickness, δ_ω, of the mixing layer. The span of the wind tunnel is 92 cm. At a downstream distance of 92 cm, the mixing-layer maximum slope thickness is about 13 cm; thus the *minimum* span of the tunnel, in units of shear-layer thickness, is 7. Twelve wires were placed laterally across the tunnel at a distance $y/\theta = 6.0$ from the vertical position marking the centre of the mixing layer. At this position, the r.m.s. turbulence level is about 2 %, and the fluctuations are irrotational most of the time; the intermittency, according to Wygnanski & Fiedler (1970), is less than 0·5 %. Figure 3 is a short time sequence illustrating the nature of the wire outputs. A brief, high-frequency burst can be seen on one channel (fourth wire from top), and this represents an outward bulge of rotational fluid. For the most part, however, the signals have only low-frequency content. These low-frequency oscillations are produced by the large-scale vortical structures passing underneath.

Hot-wire response is flat to at least 10 kHz. The hot-wire signals were first recorded on FM tape. Later these signals were digitized (12 bit conversion) and rewritten to

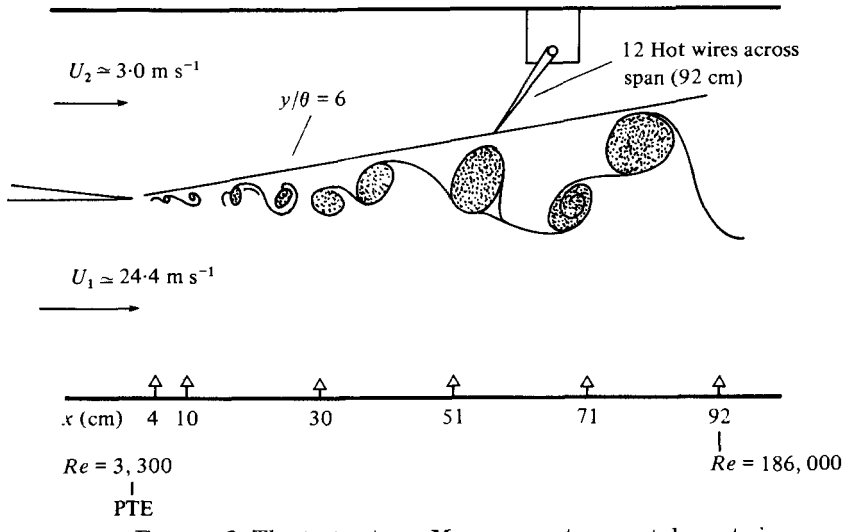

FIGURE 2. The test set-up. Measurements were taken at six downstream stations along the ray $y/\theta = 6$.

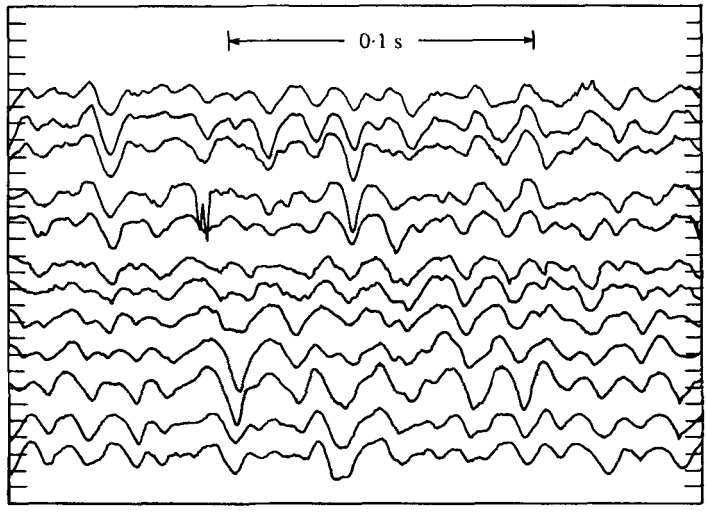

FIGURE 3. Sample output from 12 hot wires. $u_{\text{rms}}/\Delta U \simeq 1$–2 %.

digital tape. In some cases the FM tapes were played at a slower rate to expand the time scale. This was necessary since the real time digitizing rate to tape was limited to about 60 K digitizations per second (all channels). Various combinations of tape speed and digitization rate resulted in real time rates of 2000 digitizations per second to 10000 digitizations per second for each channel. The signals were digitized unfiltered, since very little, if any, high-frequency content was present.

The fluctuating voltage was defined for each hot wire by subtracting the computed mean value, and normalizing by the computed r.m.s. value. No calibration relating hot-wire fluctuation voltage to fluctuation velocity was needed because these two

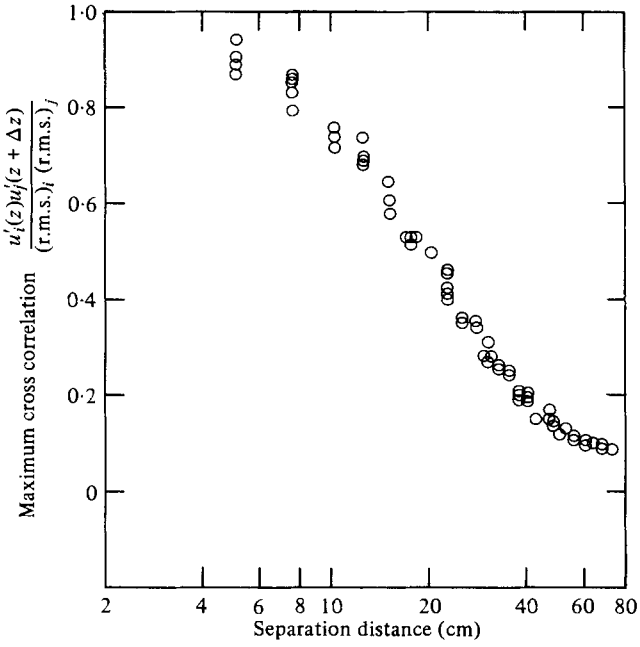

FIGURE 4. Zero time delay cross-correlations between pairs of wires at $x = 71{\cdot}1$ cm, $Re = 145\,000$, averaging time $\approx$ 2400 passage periods.

quantities are linearly related for small fluctuation amplitudes. The cross-correlation between pairs of wires separated in the spanwise direction by Δz was computed digitally at zero time delay and at a small positive and negative time delay. The maximum cross-correlation was determined by fitting a parabola through these three points. This procedure allowed for a possible (slight) shift in the position of the maximum cross-correlation away from the point of zero time delay. (Such shifts would indicate a preferred skewness in the vortex structures.) In virtually all cases these shifts were insignificant – amounting to no more than several digitizing time increments.

3. Results

Spanwise correlations

A typical set of cross-correlations at $x = 71$ cm ($Re = 145\,000$) is shown in figure 4. Each circle represents a different pair of wires. There are 66 combinations available when all twelve wires are operating. The cross-correlation values between various pairs of wires at the same separation compare well. There is a gradual decrease in correlation with increasing separation distance. At the maximum wire separation (76·2 cm), the maximum cross-correlation is still positive – having a value of approximately 0·08.

One measure of the lateral extent of the large-scale structure can be obtained by choosing a particular value for the correlation coefficient – say 40 % correlation – and plotting the spanwise separation associated with this correlation value as a function of downstream distance. The result is shown in figure 5 (the bars denote uncertainty). There is an initial decrease in the spanwise separation for 40 % correlation, and then a steady increase. The values of the separation at the last four stations lie along a

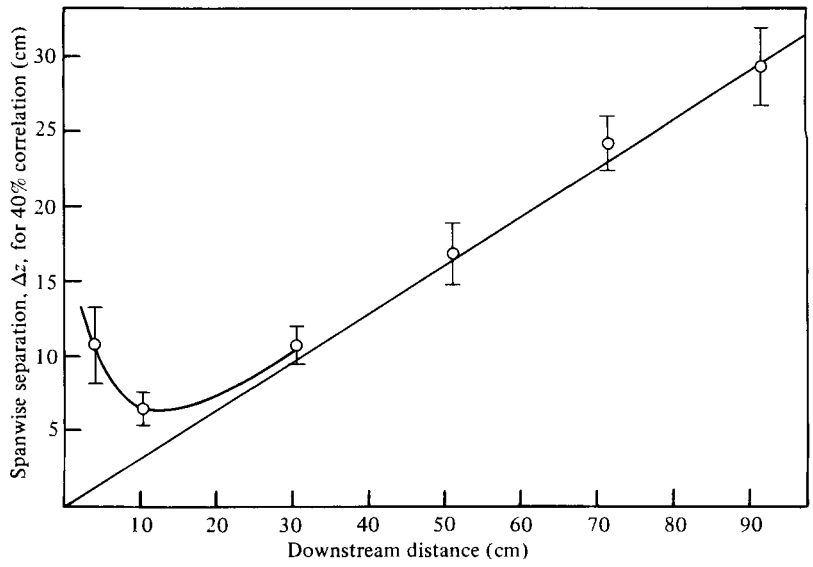

FIGURE 5. Separation distance for 40 % correlation plotted as a function of downstream position. Data is taken from plots similar to figure 4.

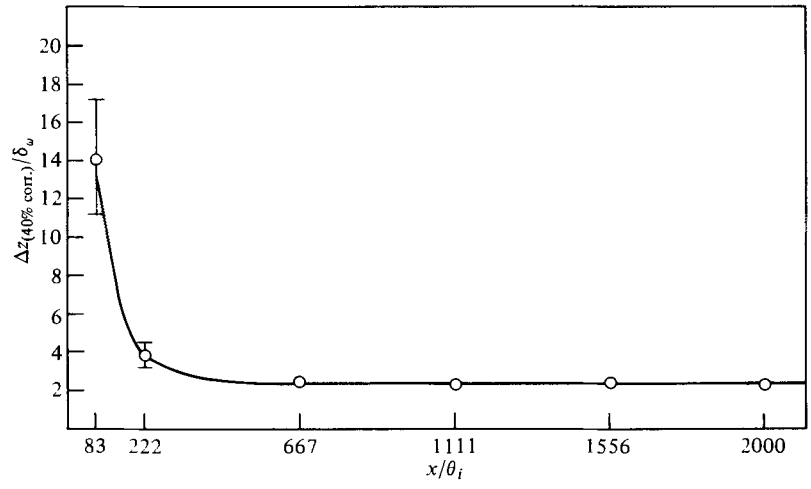

FIGURE 6. Spanwise separation for 40 % correlation, normalized by the local maximum slope thickness, δ_ω.

straight line through the origin, and this is significant. The local thickness of the mixing layer also grows linearly from the origin. The implication is, therefore, that the non-dimensional separation distance, i.e. separation distance divided by local shear-layer thickness, becomes independent of downstream position. This result is shown in figure 6 as a function of downstream distance measured in units of initial shear-layer integral thickness. Integral thickness is defined as

$$\theta = 1/(\Delta U)^2 \int_{-\infty}^{+\infty} (U_1 - u(z))\,(u(z) - U_2)\,dz,$$

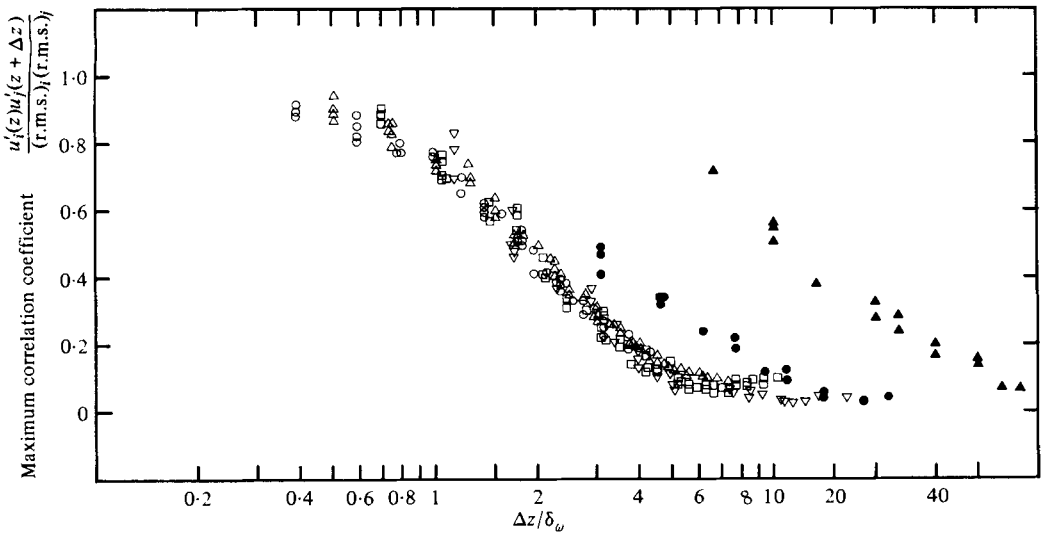

FIGURE 7. Correlation coefficients *versus* normalized spanwise co-ordinates, $\Delta z/\delta_\omega$. Symbols are: ▲, $x/\theta_i = 83$, $Re = 11000$; ●, $x/\theta_i = 222$, $Re = 23500$; ▽, $x/\theta_i = 667$, $Re = 64000$; □, $x/\theta_i = 1111$, $Re = 105000$; △, $x/\theta_i = 1556$, $Re = 145000$; ○, $x/\theta_i = 2000$, $Re = 186000$.

where U_1, U_2 are the two free-stream speeds. The separation distance for 40 % correlation asymptotes to a value of $2{\cdot}3\delta_\omega \pm 0{\cdot}25\delta_\omega$. This asymptotic value is established very near the origin, at a downstream distance of perhaps 300 initial integral thicknesses.

The choice of a particular value of correlation to define the lateral scale is artificial and not really necessary. If spanwise separation is normalized by the local shear-layer thickness, the whole of the cross-correlation distribution should become independent of downstream distance at the (four) farthest downstream stations. The properly scaled results are shown in figure 7, and indeed they do collapse onto a single asymptotic distribution. The exceptions are the first two stations, where the turbulent similarity has not yet been established. Both downstream distance and local Reynolds number corresponding to each station are shown in the caption. The rapid approach to asymptotic form is achieved (for $\lambda = 0{\cdot}8$) at a local Reynolds number of about 30 000.

The degree of lateral correlation may seem disappointingly low. At a separation of three maximum-slope thicknesses, the correlation coefficient is down to about 0·2. The 20% correlation contour encloses a region of approximately $6\delta_\omega$ in spanwise extent and approximately $2\delta_\omega$ in the streamwise direction, giving an aspect ratio of 3. Remember, though, that, in the turbulent boundary layer, the lateral correlation drops much more precipitously. At a comparable height, $y/\delta = 0{\cdot}7$, the 20% correlation contour has a spanwise extent of less than one boundary-layer thickness and a streamwise extent of perhaps 1·5 boundary-layer thicknesses, yielding an aspect ratio of approximately 0·4 (Kovasznay, Kibens & Blackwelder 1970). Thus, correlation measurements show the large-scale structure in the mixing layer to be about ten times longer in spanwise extent than comparable large structure in the turbulent boundary layer.

Again, as in the earlier example, the correlations remain positive for large separation and seem to approach a value between 0·05 and 0·1 rather than zero. If this non-zero

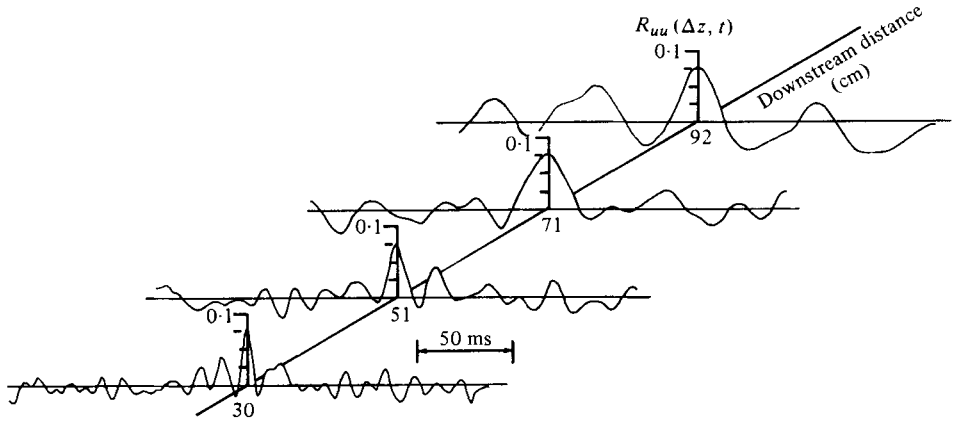

FIGURE 8. Cross-correlation functions at four downstream locations. The normalized spanwise separation, $\Delta z/\delta_\omega$, is 7 for each record.

correlation were the result of line noise common to all channels, the cross-correlations would be periodic at the frequency of 120 Hz. This is not the case, as shown in figure 8. The cross-correlations at large separation and long time delay are quasi-periodic, but the period is characteristic of the local passage period of the large-scale structure, $\delta_\omega/\frac{1}{2}(U_1+U_2)$, at each downstream station.

Visualizations of instantaneous structure

With twelve wires operating across the span, it is possible to obtain an instantaneous picture of the large-scale features. This is accomplished by first interpolating between the hot-wire locations to provide more plotting points at each instant of time. The resulting velocity field can be displayed in an isometric plot, as in figure 9 and 10. At relatively low values of the vertical gain, the view depicts an undulating surface, the features of the surface represent variations in velocity across the span as a function of time. In figure 9, the downstream position is $x/\theta_i = 1100$, and the Reynolds number is 105 000. Figure 10 shows several additional isometric plots for other downstream stations. (In comparing these, notice that the ratios of spanwise scale to longitudinal (time) scale are somewhat different for each case.)

The most striking features are the series of crests and troughs that are oriented approximately parallel to the span. These are the tracks of the large-scale vortex structures passing underneath, and are most easily followed by observing the dark ridges (corresponding to the back sides of the undulations). The large majority of the observed ridges span the wind tunnel, and they are often skewed rather than being perfectly two-dimensional. Branching also occurs such that two ridges merge to form a single ridge over a portion of the span. The continuity or 'connectedness' of the ridges, and the relative scarcity of 'ends' or terminations, is consistent with the interpretation of underlying vortex structure. Since vortex lines cannot end in the flow, terminations are rare and, when they occur, must correspond to a local redistribution, or smearing out, of the vorticity.

The skewness and branching of ridges, we associate with pairing interactions between vortices. These interactions are the result of an instability which, in its

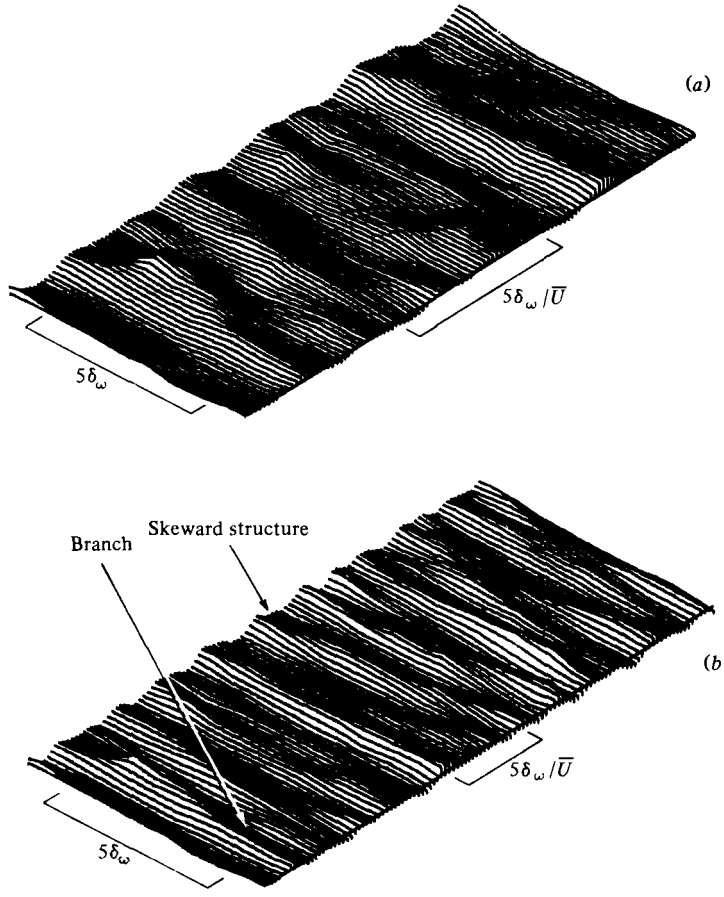

FIGURE 9. Instantaneous velocity surfaces at $x = 71{\cdot}1$ cm as a function of span and time. The time scale is decreased by a factor of 2 in (*b*).

simplest form, was discussed by Lamb (1945). Any small departure from uniformity in spacing along the span of the vortex will be amplified as the interaction proceeds and might easily lead to the observed skewness. Branching can be viewed as an extreme form of skewness.

The concept of a big eddy as an isolated 'blob' having a lateral extent of approximately $6\delta_\omega$ would be consistent with the correlation measurements, but *not* consistent with the visualizations of instantaneous structure. Thus, the isocorrelation contours should not be interpreted too literally. In fact, the vortex features are (almost always) much longer than $6\delta_\omega$. The observed reduction in spanwise correlation is a direct result of vortex skewness, and hence is associated with the pairing interactions between adjacent features. The association of spanwise correlation (or lack of correlation) with the large-scale interactions was noted by one of the referees. He suggested that since the spanwise separation for fixed correlation and the mixing-layer thickness *both* grow linearly with downstream distance, it is reasonable to assume the effects arise from a common cause.

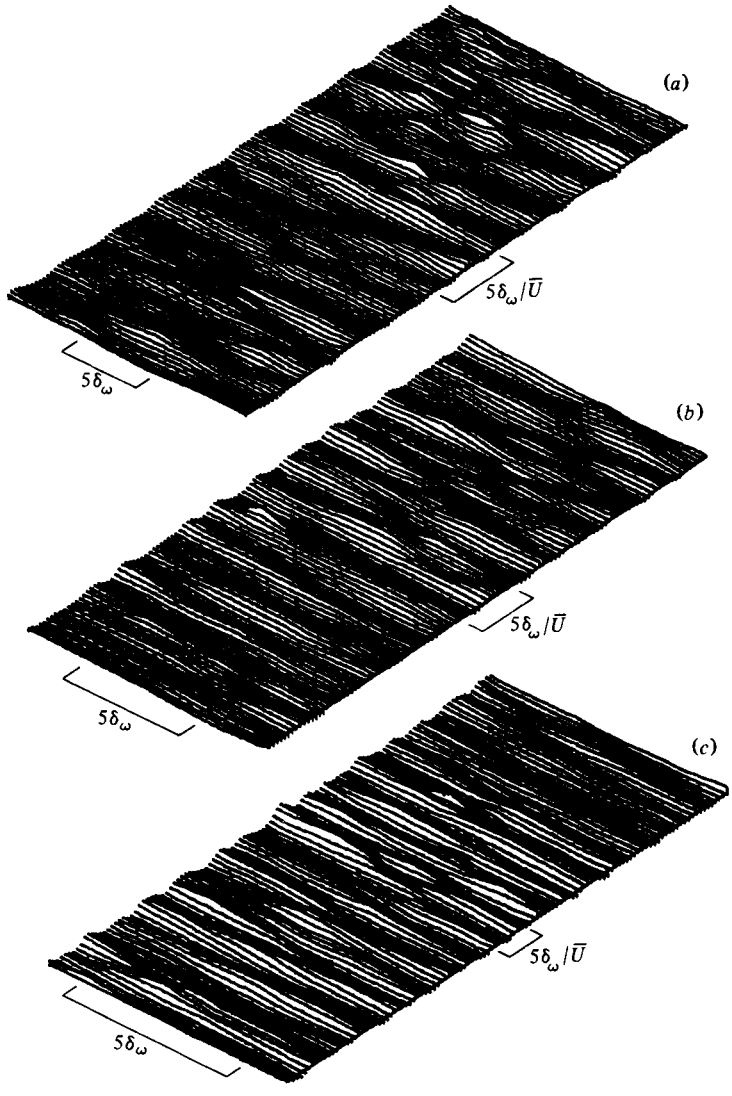

FIGURE 10. Instantaneous velocity surfaces as a function of span and time. (*a*) $x = 30{\cdot}0$ cm, $Re = 64000$; (*b*) $x = 51{\cdot}0$ cm, $Re = 105000$; (*c*) $x = 71{\cdot}1$ cm, $Re = 145000$.

4. Concluding remarks

The spanwise cross-correlation measurements have shown that, beyond a certain initial-development length, the large structure approaches an asymptotic scale when normalized by the local mixing-layer thickness. For our large velocity ratio, $\lambda = 0{\cdot}8$, the achievement of self-similarity is essentially completed at a Reynolds number of 30 000 or, equivalently, at $x/\theta_i = 300$. Beyond this point no further changes in structure occur. This result convincingly demonstrates the *persistence* of these large features.

Isometric visualizations of the velocity field were used to form a more complete picture of spanwise structure. The large-scale vortex features are not precisely two-dimensional for they are skewed and have multiple branches. The principal alignment is in the *spanwise* direction, however, and the majority of the structures can be traced

across the *full width* of the wind tunnel. We would be inclined to describe this large structure as quasi two-dimensional.

It would be useful to attempt a comparison between the present results and several of the experiments mentioned earlier. This must be done with caution, however. The position, x_t, where self-similar spanwise structure is achieved can be expected to depend upon two parameters as follows, $x_t/\theta_i = f(\Delta U\theta_i/\nu, \lambda)$. Rigorous comparisons between various experiments require, among other things, a knowledge of this relationship; but it cannot be determined from the present measurements since only one value each of λ and θ_i was involved. Tentative conclusions might still be made in cases where the parameter ranges are not too dissimilar from the present values.

Some of the experiments of Brown & Roshko (1974), and the additional experimental results discussed by Roshko (1976) (cf. his figure 3), do extend well beyond the Reynolds number, $\Delta U\delta_\omega/\nu = 3 \times 10^4$, here shown to be necessary for the attainment of asymptotic spanwise structure. The extreme two-dimensionality of the large features in some of these plan-view photographs may suggest a dependence of x_t on λ (0·45 *versus* our value of 0·8), or it may simply be due to the limited spanwise extent of the flow. In either case, the presence of an occasional end or slight skewness cannot be expected to change the picture dramatically. The visualizations can legitimately be viewed as representing a typical cross-section through a series of large-scale vortex structures.

The smoke observations reported by Chandrsuda *et al.* (1978) for $\lambda = 1{\cdot}0$ appear to be upstream of our asymptotic limit. The maximum Reynolds number in the photographs (Chandrsuda *et al.* 1978, figures 2 and 3) is approximately 8000 based on the local maximum slope thickness. From the results of our figure 5, the region characterized by the Reynolds number range 8000–20 000 shows a rapid decrease in the large-structure scales, and the least degree of correlation at fixed spanwise separation of any downstream region in the mixing layer. Thus, the photographs in Chandrsuda *et al.* which show an increase in three-dimensionality in this region are not inconsistent with our quantitive results. Based solely on the photographs, however, one is tempted to conclude that the flow farther downstream will be even more three-dimensional. Our more extensive results show this conclusion to be incorrect. The degree of correlation at fixed separation beyond this region actually increases as figure 5 shows.

The work of Wygnanski *et al.* (1979) is primarily an intercomparison experiment using various means to modify the initial mixing layer. The Reynolds number based on the mixing-layer thickness for their measurements at 110 cm downstream is approximately 50 000, and their value of λ is 0·40. The surprising thing about their results is the magnitudes of the measured spanwise correlations. Making an estimate for the maximum slope thickness, δ_ω, at 110 cm, figure 2 of Wygnanski *et al.* shows a correlation coefficient $R_{uu} \approx 0{\cdot}7$ for a value $\Delta z/\delta_\omega \approx 8$–9. This correlation is significantly higher than any we measured. The explanation for this difference may lie in our lack of knowledge of the variation of the asymptotic limit as a function of λ and $\Delta U\theta_i/\nu$. We are presently designing an experiment to determine this functional relationship.

The authors wish to acknowledge the financial support of the Office of Naval Research under grant N00014-76-C-02111, and the National Science Foundation under grant ENG 78-02249. Prof. R. E. Kaplan is responsible for the isometric plotting program, and for the digitizing capability.

REFERENCES

BROWAND, F. K. & LATIGO, B. O. 1979 The growth of the two-dimensional mixing layer from a turbulent and non-turbulent boundary layer. *Phys. Fluids* **92**, 1011–1019.

BROWN, G. & ROSHKO, A. 1974 On density effects and large structure in turbulent mixing layers. *J. Fluid Mech.* **83**, 641–671.

CHANDRSUDA, C., MEHTA, R. D., WEIR, A. D. & BRADSHAW, P. 1978 Effects of free-stream turbulence on large structure in turbulent mixing layers. *J. Fluid Mech.* **85**, 693–704.

DIMOTAKIS, P. E. & BROWN, G. 1976 The mixing layer at high Reynolds number: large structure dynamics and entrainment. *J. Fluid Mech.* **78**, 535–560.

KOVASZNAY, L. S. G., KIBENS, V. & BLACKWELDER, R. 1970 Large-scale motion in the intermittent region of a turbulent boundary layer. *J. Fluid Mech.* **41**, 283–325.

LAMB, H. 1945 *Hydrodynamics*, pp. 224–229. New York: Dover.

ROSHKO, A. 1976 Structure of turbulent shear flows. *A.I.A.A. J.* **14**, 1349–1357.

WYGNANSKI, I. & FIEDLER, H. E. 1970 The two-dimensional mixing region. *J. Fluid Mech.* **41**, 327–361.

WYGNANSKI, I., OSTER, D., FIEDLER, H. & DZIOMBA, B. 1979 On the perseverance of a quasi two-dimensional eddy-structure in a turbulent mixing layer. *J. Fluid Mech.* **92**, 1–16.